Radboud Repository

Radboud University Nijmegen

PDF hosted at the Radboud Repository of the Radboud University Nijmegen

The following full text is a publisher's version.

For additional information about this publication click this link.
http://hdl.handle.net/2066/50769

Please be advised that this information was generated on 2019-01-21 and may be subject to change.

MOLECULAR AND CELLULAR BIOLOGY, Jan. 2006, p. 303–312 Vol. 26, No. 1
0270-7306/06/$08.00+0 doi:10.1128/MCB.26.1.303–312.2006
Copyright © 2006, American Society for Microbiology. All Rights Reserved.

Direct Interaction with Rab11a Targets the Epithelial Ca^{2+} Channels TRPV5 and TRPV6 to the Plasma Membrane

Stan F. J. van de Graaf, Qing Chang, Arjen R. Mensenkamp, Joost G. J. Hoenderop, and René J. M. Bindels*

Department of Physiology, Nijmegen Centre for Molecular Life Sciences, Radboud University Nijmegen Medical Centre, Nijmegen, The Netherlands

Received 16 June 2005/Returned for modification 18 July 2005/Accepted 3 October 2005

TRPV5 and TRPV6 are the most Ca^{2+}-selective members of the transient receptor potential (TRP) family of cation channels and play a pivotal role in the maintenance of Ca^{2+} balance in the body. However, little is known about the mechanisms controlling the plasma membrane abundance of these channels to regulate epithelial Ca^{2+} transport. In this study, we demonstrated the direct and specific interaction of GDP-bound Rab11a with TRPV5 and TRPV6. Rab11a colocalized with TRPV5 and TRPV6 in vesicular structures underlying the apical plasma membrane of Ca^{2+}-transporting epithelial cells. This GTPase recognized a conserved stretch in the carboxyl terminus of TRPV5 that is essential for channel trafficking. Furthermore, coexpression of GDP-locked Rab11a with TRPV5 or TRPV6 resulted in significantly decreased Ca^{2+} uptake, caused by diminished channel cell surface expression. Together, our data demonstrated the important role of Rab11a in the trafficking of TRPV5 and TRPV6. Rab11a exerts this function in a novel fashion, since it operates via direct cargo interaction while in the GDP-bound configuration.

TRPV5 and TRPV6 (TRPV5/6) form a distinct group of highly Ca^{2+}-selective channels belonging to the transient receptor potential (TRP) channel superfamily. This family fulfills a plurality of physiological functions, which vary from phototransduction, nociception, olfaction, and heat and cold sensation to epithelial Ca^{2+} transport (28). TRPV5 and TRPV6 mediate the rate-limiting luminal influx step of transcellular Ca^{2+} transport (19, 23). Therefore, understanding the regulation of these channels is of utmost importance for our insight into Ca^{2+} homeostasis. TRPV5 and TRPV6 display constitutive activity (43), suggesting that channel abundance at the cell surface is of crucial importance for regulation of Ca^{2+} influx via these channels. It is becoming increasingly evident that channel trafficking is essential in determining the activity of TRP proteins (2, 3, 26, 36, 46). For instance, inducible vesicular translocation and plasma membrane insertion have been described for several TRP channels, i.e., TRPV2, TRPC3, TRPC5, and TRPL. This trafficking process stimulated Ca^{2+} influx from the extracellular compartment essential to growth factor-induced (3, 26), carbachol-induced (36), or light-induced (46) signaling. However, little is known about the molecular mechanisms involved in trafficking to the plasma membrane of TRP channels in general and of TRPV5 and TRPV6 in particular.

Several protein families have been described as playing key roles in cargo trafficking to and from specific cellular compartments, including the plasma membrane. One of these families consists of the Rab GTPases. The ability to act as molecular switches that cycle between GTP- and GDP-bound states underlies the functionality of this family. Many Rab proteins show a distinct subcellular localization, making them ideal candidates to govern the specificity of vesicle trafficking, most likely by cooperatively operating with other proteins (16, 47). Further characterization of the largely elusive mechanism underlying the function of Rab proteins in ion channel trafficking could further contribute to the already enigmatic Rab-dependent regulation of cargo trafficking in the highly organized cellular transport machinery.

The aim of this study was to identify regulatory proteins directly interacting with TRPV5 or TRPV6. Using biochemical, histological, and functional analyses, we demonstrate a novel operation mode for Rab11a in the regulation of TRPV5 and TRPV6 trafficking to the plasma membrane requiring direct interaction with these cargo molecules.

MATERIALS AND METHODS

DNA constructs and cRNA synthesis. The carboxyl termini of mouse TRPV5 and TRPV6 and deletion mutants of TRPV5 in pGEX6p-2 were obtained as described previously (41). A vesicular stomatitis virus (VSV) tag-encoding oligonucleotide duplex (sense, 5′-CATGGCATACACTGATATCGAAATGAA CCGCCTGGGTAAGGCGCGCCTT-3′; and antisense, 5′-CTAGAAGGCGCG CCTTACCCAGGCGGTTCATTTCGA TATCAGTGTATGC-3′) was inserted into the NcoI/XbaI restriction sites of the pTLN oocyte expression vector. Rab11a was cloned into this construct by PCR (forward primer, 5′-GGCGCG CCTTGGCACCCGCGACGACGAGTAC-3′; and reverse primer, 5′-GTGAAC TTGCGGGGTTTTTCAGTATCTACGA-3′) with the pACT2 construct as a template and was subsequently subcloned into pGEX6p2 (Amersham Biosciences, Uppsala, Sweden) and pCB7 (4). MluI and SalI sites were introduced into the lentivirus transfer vector pLV-CMV-GFP (35) by site-directed mutagenesis replacing the green fluorescent protein (GFP) stop codon. Rab11aS25N was subsequently cloned into these sites by PCR using the forward primer 5′-AGC ACGCGTGGCACCCGCGACGACGA-3′ and the reverse primer 5′-ACAGTC GACTTAGATGTTCTGACAGCACTG-3′. TRPV5 was cloned into enhanced GFP (EGFP)-C1 (Clontech Palo Alto, CA) by PCR (forward primer, 5′-TCCGGA CGGGGGGGGATGGGGGCCTGTCCACCC-3′; and reverse primer, 5′-CCG GTGGATCCTGATCAG-3′). The construct encoding DsRed-fused Rab11a was generously provided by U. Rescher (University of Muenster, Muenster, Germany) and S20V and S25N mutants were subsequently obtained by site-directed mutagenesis. All constructs were verified by sequence analysis. Oocyte expres-

* Corresponding author. Mailing address: 286 Cell Physiology, Radboud University Nijmegen Medical Centre, P.O. Box 9101, NL-6500 HB Nijmegen, The Netherlands. Phone: 31-24-3614211. Fax: 31-24-3616413. E-mail: r.bindels@ncmls.ru.nl.

sion constructs were linearized, and TRPV5, TRPV6, and Rab11a cRNA were synthesized in vitro with SP6 RNA polymerase as described previously (22).

Yeast two-hybrid system. Yeast was subsequently transformed with pAS-1 containing the TRPV6 carboxyl terminus, and a mouse kidney cDNA library (Clontech, Palo Alto, CA) was present in the pACT2 vector. Screening of the library was performed as described previously (41). Yeast two-hybrid results were confirmed using purified library plasmids, and negative controls were performed by replacing a binding partner by either a pAS-1 construct containing the amino terminus (amino acids 1 to 53) of rat gamma epithelial Na^+ channel (γENaC) or the empty pACT2 vector.

GST-TRPV5/6 fusion protein and interaction assays. pGEX6p-2 constructs were transformed in *Escherichia coli* BL21, and glutathione *S*-transferase (GST) fusion proteins were expressed and purified according to the manufacturer's protocol (Amersham Biosciences, Piscataway, NJ). GST-Rab proteins were prepared in GTP- or GDP-bound conformation as previously described (11). Rab11a S25N was cleaved from GST with Precission protease (Amersham Biosciences), concentrated with Centriprep YM10 (Millipore, Amsterdam, The Netherlands), and checked by sodium dodecyl sulfate-polyacrylamide gel electrophoresis. [^{35}S]methionine-labeled full-length Rab11a or TRPV5/TRPV6 protein was prepared with a reticulocyte lysate system (Promega, Madison, WI). HEK293 cells were transfected with Rab11a, Rab22b, or Rab7 constructs and lysed in pull-down buffer (20 mM HEPES, 100 mM NaCl, 5 mM $MgCl_2$, 1 mM dithiothreitol, 100 μM GTP or GDP, and 0.4% [vol/vol] Triton X-100 [pH 7.5]). Rab proteins, TRPV5, or TRPV6 was added to GST or GST fusion proteins immobilized on glutathione-Sepharose 4B beads (Amersham Biosciences) in pull-down buffer and incubated for 2 h at room temperature. After being extensively washed, bound proteins were eluted with sodium dodecyl sulfate-polyacrylamide gel electrophoresis loading buffer and visualized by autoradiography or immunoblotting using rabbit anti-Rab11 (Zymed, San Francisco, CA), monoclonal anti-VSV (Sigma, St Louis, MO, for Rab11 and Rab22b), or anti-myc (Santa Cruz Biotechnology, Santa Cruz, CA, for Rab7). The quality and quantity of GST or GST-fused proteins were routinely analyzed by Coomassie staining.

Coimmunoprecipitation. *Xenopus laevis* oocytes were coinjected with 10 ng TRPV5 and 10 ng Rab11a S25N cRNA as previously described (22). After 48 h, injected oocytes were lysed in sucrose buffer containing 20 mM Tris (pH 7.4), 5 mM EDTA, 135 mM NaCl, 0.1% (vol/vol) NP-40, 0.5% (wt/vol) sodium desoxycholate, and 10% (wt/vol) sucrose; centrifuged at 100 g for 5 min; and subsequently incubated on ice for 60 min. The lysates were centrifuged for 30 min at 16,000 × *g*, and supernatants were incubated with monoclonal anti-hemagglutinin (HA) antibodies (Sigma, St Louis, MO) immobilized on protein A-agarose beads (Kem-En-Tec A/S, Copenhagen, Denmark) for 16 h at 4°C. Immunoprecipitated proteins were analyzed by immunoblot analysis using rabbit anti-Rab11a antibodies.

CNT and CCD primary cell culture and transepithelial Ca^{2+} transport. Connecting tubules (CNT) and cortical collecting ducts (CCD) were immunodissected from the kidney cortexes of New Zealand White rabbits (±0.5 kg) and placed in primary culture on permeable filters (0.33 cm^2; Costar), and transepithelial Ca^{2+} transport was measured as described previously (20) in the presence or absence of 1 μM ruthenium red (Sigma, St Louis, MO). Cells were subsequently fixed in 3% (wt/vol) paraformaldehyde in phosphate-buffered saline (PBS) for 30 min at 4°C.

Lentiviral infection of primary CNT/CCD cells. Third-generation lentiviruses were produced by cotransfection of the packaging vectors pRSV-Rev, pMDL g/p RRE, and pMD2G from Tronolab (Lausanne, Switzerland) and the transfer vector into human embryonic kidney 293T cells as described previously (12). The titer was determined by a p24 human immunodeficiency virus enzyme-linked immunosorbent assay (Murex Diagnostics, Dartford, United Kingdom). Primary rabbit CNT/CCD cells were infected with lentivirus immediately before being plated in the presence of Polybrene (8 μg/ml) using 1 or 10 virus particles per cell (multiplicity of infection of 1 or 10). Virus was removed after 24 h. Transepithelial Ca^{2+} transport was measured 6 days postinfection in the presence of 10 μM forskolin as described before (20).

Immunofluorescence microscopy. Immunohistochemistry of mouse kidney sections was performed as described previously (18) using affinity-purified guinea pig antiserum against TRPV5 and rabbit anti-Rab11 antibodies. Serial sections were incubated with rabbit anti-TRPV6 or rabbit anti-Rab11a antibodies. *Xenopus laevis* oocytes were injected with 5 ng HA-tagged TRPV5 cRNA or 5 ng Flag-tagged TRPV6 cRNA with or without 10 ng Rab11a cRNA. Two days after injection, immunocytochemistry was performed as previously described (22) using anti-HA or rabbit anti-TRPV6 (dilution, 1:400). HeLa cells were grown on coverslips and transfected with Effectene (QIAGEN, Valencia, CA) according to the manufacturer's protocol. Sixteen hours after transfection, cells were fixed with 4% (wt/vol) paraformaldehyde in PBS for 10 min at room temperature, incubated with 50 mM NH_4Cl in PBS for 5 min, washed with PBS, and mounted in Mowiol containing 4% (wt/vol) *n*-propyl-gallate as an antifade agent. Cells fixed on permeable filter supports were stained with guinea pig anti-TRPV5, rabbit anti-Rab11, and appropriate secondary antibodies coupled to Alexa 488 or Alexa 596 and mounted in Mowiol. The cell surface was visualized by biotinylation from the apical and basolateral compartment, followed by incubation with streptavidin-Oregon green 488, essentially as previously described (44). This procedure predominantly stained the basolateral cell surface. Images were taken sequentially with a Bio-Rad MRC 1024 confocal microscope or with a Zeiss LSM510 Meta confocal microscope, emitting at 488 nm and 543 nm with a 30-mW argon laser and a 1-mW helium-neon laser. Emissions were collected using a 505- to 530-nm band-pass filter or a 560-nm-long pass filter. XZ scans were constructed from 35 confocal optical sections (0.2 μm apart). All negative controls, including noninjected oocytes or sections incubated with preimmune serum or conjugated antibodies alone, were devoid of staining.

$^{45}Ca^{2+}$ uptake assay. *Xenopus laevis* oocytes were coinjected with TRPV5 or TRPV6 and Rab11a cRNA. Ca^{2+} uptake was determined 2 days after injection as described previously (21).

Plasma membrane isolation. *Xenopus laevis* oocytes were injected with 5 ng TRPV5 cRNA only or coinjected with 5 ng TRPV5 and 10 ng Rab11a cRNA. After 48 h, follicle membranes were manually removed, and plasma membranes were isolated from 12 oocytes as described previously (25).

Statistical analysis. In all experiments, the data are expressed as means ± standard error of the mean. Overall statistical significance was determined by analysis of variance. *P* values of <0.05 were considered significant.

RESULTS

Identification of Rab11a as a TRPV5- and TRPV6-associated protein. Using the carboxyl terminus of TRPV6 as bait to screen a mouse kidney cDNA library by the yeast two-hybrid technique, we isolated full-length Rab11a, a member of the Rab family of small GTPases, as a TRPV6-interacting protein. Rab11a strongly interacted with TRPV6 (Fig. 1A), whereas β-galactosidase activity was not observed with the negative control in the absence of prey or after cotransformation of the bait with the empty pACT2 (prey) vector.

The interaction between TRPV6 and Rab11a was further substantiated by GST pull-down assays. In vitro-translated [^{35}S]methionine-labeled TRPV6 strongly interacted with Rab11a S25N, a mutant deficient in GTP binding. Binding to wild-type (WT) Rab11a was moderate; only minor levels of binding to Rab11a S20V, a GTPase-deficient Rab11a mutant (45), were observed (Fig. 1B). Identical results were obtained with [^{35}S]methionine-labeled TRPV5 (Fig. 1B). The reverse binding reaction, using GST, the GST-TRPV5 carboxyl terminus, or the GST-TRPV6 carboxyl terminus incubated with in vitro-translated [^{35}S]methionine-labeled Rab11a S20V or Rab11a S25N mutants, confirmed the TRPV5- and TRPV6-binding specificity for Rab11a S25N (Fig. 1D). GST alone failed to show any binding under all conditions. The integrity and quantity of the GST fusion proteins were analyzed by Coomassie staining and show that equivalent amounts of protein were used in these assays (Fig. 1C and E). To further assess the Rab11a interaction, HA-tagged TRPV5 and Rab11a S25N were coexpressed in *Xenopus laevis* oocytes and subjected to immunoprecipitation with monoclonal anti-HA antibodies. HA-tagged TRPV5 was specifically precipitated with these monoclonal antibodies, as indicated by the specific bands at ~70 kDa for the core-glycosylated TRPV5 and ~90 kDa for the complex-glycosylated TRPV5 (Fig. 1F). Rab11a S25N was coprecipitated with TRPV5 from these oocytes, as represented by an immunopositive band of ~25 kDa (Fig. 1G).

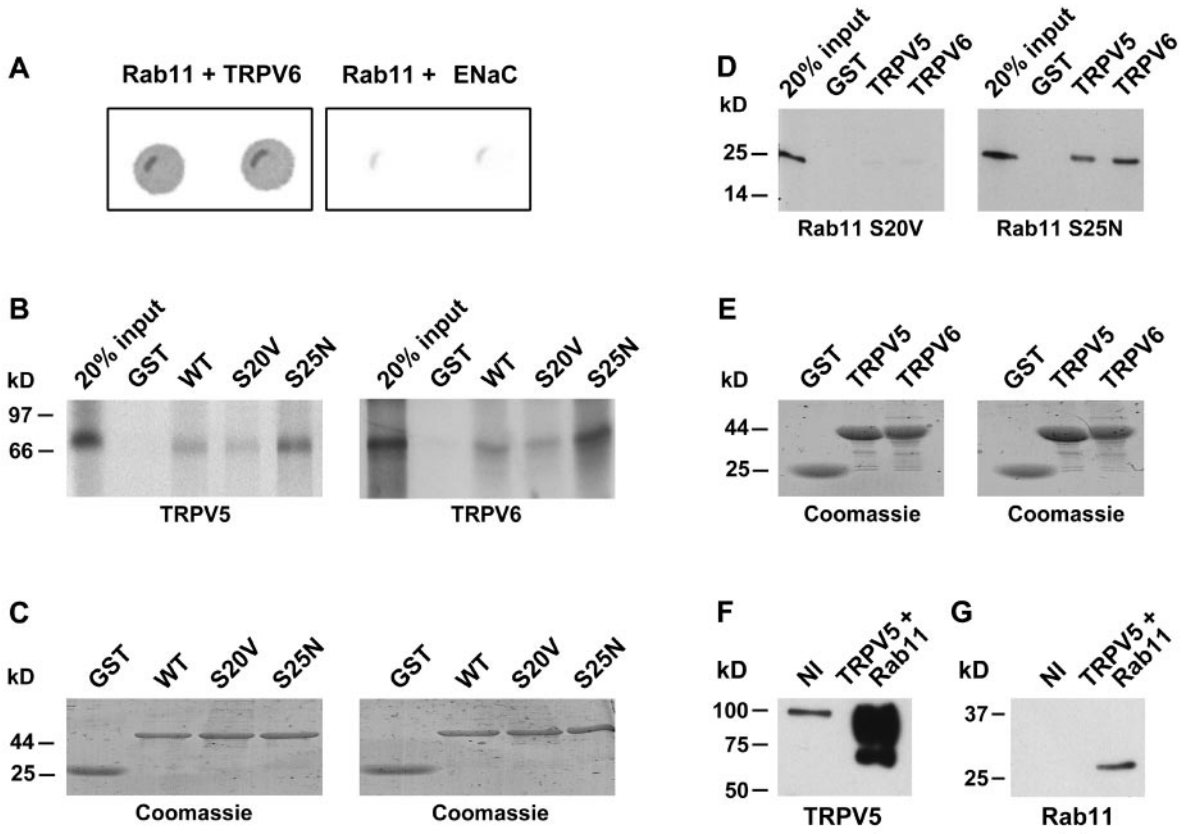

FIG. 1. Interaction of TRPV5 and TRPV6 with Rab11a. (A) The carboxyl terminus of TRPV6 or γENaC and full-length Rab11a were cotransformed into the Y153 yeast strain and grown on media without tryptophan and leucine. β-Galactosidase activity was determined for TRPV6- and Rab11a-cotransformed yeast, and γENaC- and Rab11a-cotransformed yeast was used as a negative control. Two representative colonies are depicted. (B) [^{35}S]methionine-labeled TRPV5 (left) or TRPV6 (right) was incubated with GST-Rab11a WT, GTP-locked mutant Rab11a (S20V), GDP-locked Rab11a (S25N), or GST alone immobilized on glutathione-Sepharose 4B beads. (C) Coomassie staining of the gels shows equal expression of GST, GST-fused Rab11a WT S20V, or S25N. (D) [^{35}S]methionine-labeled Rab11a S20V or Rab11a S25N was incubated with GST-TRPV5, GST-TRPV6, or GST immobilized on glutathione-Sepharose 4B beads. Both TRPV5 and TRPV6 strongly interacted with Rab11a S25N, whereas no binding to Rab11a S20V was observed. (E) Coomassie staining of the gels demonstrating similar amounts of GST, GST fused to the carboxyl terminus of TRPV5, or GST fused to the carboxyl terminus of TRPV6. (F and G) *Xenopus laevis* oocytes were injected with Rab11a S25N or coinjected with HA-tagged TRPV5 and Rab11a S25N cRNAs. Oocyte lysates were subjected to immunoprecipitation using monoclonal anti-HA antibodies. The precipitated sample was immunoblotted for the presence of TRPV5 (F) or coprecipitated Rab11a (G).

Subsequently, the specificity for Rab11a was determined using distant members of the Rab family of GTPases. Rab22b S19N and Rab7 T22N, both GTP-binding-deficient Rab proteins, did not bind TRPV5 and TRPV6, indicating the specificity of the interaction of TRPV5/6 with Rab11a (Fig. 2A). GST, GST-fused TRPV5, and GST-fused TRPV6 were present in equal amounts, as demonstrated by Coomassie staining (Fig. 2B). GST alone did not show any binding under these conditions. To investigate whether the association between Rab11a and the epithelial Ca^{2+} channels was direct, recombinant Rab11a S25N was purified as a GST fusion protein and subsequently cleaved from GST using Precission protease. The purity of recombinant Rab11a was analyzed by Coomassie staining (Fig. 2C, right). Purified Rab11a S25N displayed similar TRPV5-binding efficiencies (Fig. 2C), demonstrating that the interaction was direct and did not require additional proteins.

Colocalization of Rab11a with TRPV5 and TRPV6. Subsequently, we examined whether TRPV5 colocalized with WT Rab11a and the GTP- and GDP-locked Rab11a mutants. To this end, HeLa cells were transiently transfected with constructs encoding EGFP-tagged TRPV5 and DsRed-tagged Rab11a (WT, S20V, or S25N) and the subcellular localization of TRPV5 and Rab11a was visualized by confocal laser scanning microscopy. TRPV5 was clearly present in many vesicles distributed throughout the cytoplasm, where it showed prominent colocalization with wild-type Rab11a (Fig. 3A) and to a lesser extent in the endoplasmic reticulum. Similarly, TRPV5 also colocalized with Rab11a S20V, the GTP-locked form of Rab11a, in vesicular structures, strongly resembling the pattern observed with wild-type Rab11a (Fig. 3B). Interestingly, a significant vesicular colocalization of TRPV5 was observed with GDP-locked Rab11a S25N (Fig. 3C), as opposed to the dispersed localization of Rab11a S25N observed previously (32, 39). These findings are in line with our GST pull-down and coimmunoprecipitation results and suggest that GDP-bound Rab11a is at least in part vesicle associated in TRPV5-expressing cells. DsRed-fused wild-type Rab4 showed little or no colocalization with TRPV5, indicating that this channel is particularly enriched in the Rab11a-positive compartment (Fig. 3D). Furthermore, YFP-fused TRPV2 did not colocalize with

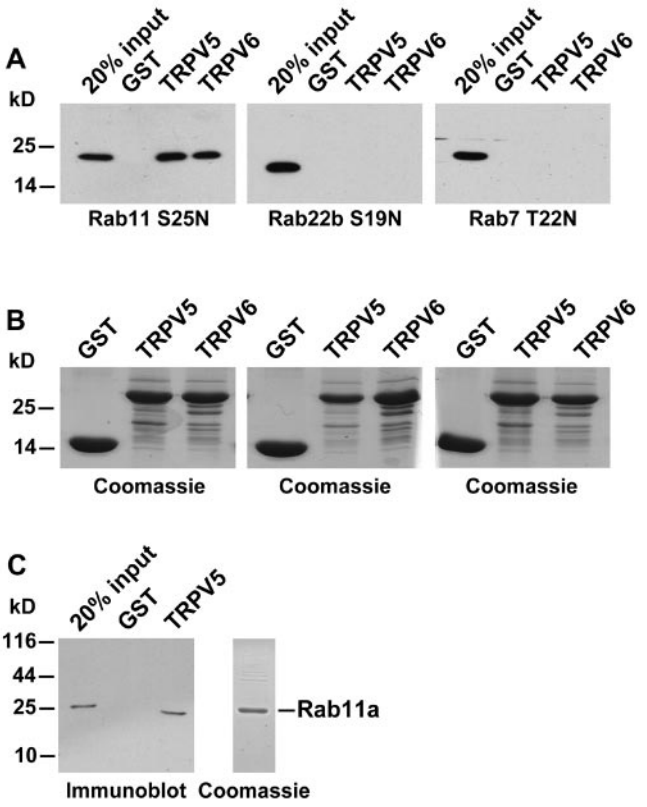

FIG. 2. (A) VSV-tagged Rab11a S25N or Rab22b S19N and myc-tagged Rab7 T22N were transiently expressed in HEK293 cells and incubated with GST or GST fused to the carboxyl terminus of TRPV5 or TRPV6, and interactions were analyzed by immunoblot analysis using monoclonal anti-VSV or anti-Myc. (B) Coomassie staining of the precipitated GST fusion proteins, demonstrating equal amounts of GST or GST fused to the carboxyl terminus of TRPV5 or TRPV6. (C) Rab11a S25N was expressed in bacteria as a GST fusion protein, GST was cleaved using Precission protease, and purified Rab11a S25N was incubated with immobilized and purified GST-TRPV5. Bound Rab11a was detected by immunoblot analyses using anti-Rab11 antibodies (left). The integrity and purity of Rab11a S25N were verified by Coomassie staining (right).

Rab11a, but showed a strong plasma membrane staining (Fig. 3E). A clear plasma membrane localization of TRPV5 was not observed in either of the conditions, although a significant TRPV5-mediated Ca^{2+} influx was measured in TRPV5-transfected HeLa cells compared to nontransfected cells (data not shown). This suggests that a small number of TRPV5 channels are present at the plasma membrane to facilitate Ca^{2+} influx but prevent cytosolic overload with Ca^{2+}. To determine whether the interaction can also occur under physiological conditions, the cellular colocalization of endogenous TRPV5 and TRPV6 with endogenous Rab11a was investigated. Immunopositive staining for Rab11a colocalized with TRPV5 in specific kidney tubules, previously identified as distal convoluted and CNT (Fig. 4A) (18). Furthermore, serial sections were stained for the presence of Rab11a and TRPV6, revealing coexpression of both proteins in the luminal domains of CNT and CCD (Fig. 4B) (29). More-detailed localization studies were subsequently performed with primary cultures of CNT and CCD cells, immunodissected from rabbit kidney. These cells exhibited net apical-to-basolateral Ca^{2+} transport, indicating the integrity and functionality of the preparation. Ca^{2+} transport was blocked (from 63 ± 3 to 5 ± 2 nmol/cm^2/h) by ruthenium red, a polycationic dye that blocks TRPV5 activity with an 50% inhibitory concentration of 111 nM (Fig. 4F) (30). TRPV5 staining localized predominantly to the apical side of the cell and was absent from the basolateral membrane that is in line with its physiological function as apical Ca^{2+} influx channel (Fig. 4E). Importantly, TRPV5 immunopositive staining overlapped with that of Rab11a in vesicular structures (Fig. 4C). Analysis of z-stacks of these cells (Fig. 4D) combined with plasma membrane staining (Fig. 4E) confirmed the colocalization of Rab11a and TRPV5 in a subapical region. Thus, these findings further substantiated the physiological relevance of the interaction between the epithelial Ca^{2+} channels and Rab11a.

Characterization of the Rab11a-binding site in TRPV5. To map the Rab11a-binding site, a series of deletion mutants of the carboxyl terminus of TRPV5 was constructed as depicted in Fig. 5A. These mutants were expressed and purified as GST fusion proteins and incubated with in vitro-translated Rab11a S25N. Rab11a interacted with TRPV5 truncates up to position 601, narrowing the binding site to a helical region of 29 amino acids. Two truncated TRPV5 mutants, containing stop codons at position 596 or 591, failed to coprecipitate Rab11a (Fig. 5B). Therefore, the region between amino acids 595 and 601 of TRPV5 was essential for Rab11a binding. Subsequently, this region, corresponding to the amino acid sequence MLERK, was mutated into glycines (designated 595-5G-601), and the binding of Rab11a was reanalyzed by GST pull-down. The interaction between Rab11a and the mutant 595-5G-601 TRPV5 was significantly decreased, further indicating the relevance of this MLERK domain for Rab11a interaction (Fig. 5B). Of note, the binding region for the previously identified TRPV5-interacting protein S100A10 is located upstream of this Rab11a-binding region (41); the T593A (amino acid numbering according to the mouse sequence; accession number NP001007573) mutation in TRPV5, which is crucial for S100A10 binding, had no effect on binding of Rab11a (data not shown), indicating the specificity of the identified region. GST alone did not bind Rab11a, and in vitro-translated Rab22b did not show any affinity for TRPV5 under these conditions (Fig. 5C). Importantly, the diminished binding of Rab11a to the TRPV5 595-5G-601 mutant was accompanied by an impaired trafficking of TRPV5, as was demonstrated by immunocytochemical analysis of *Xenopus laevis* oocytes injected with TRPV5 wild-type or 595-5G-601 mutant cRNA. Wild-type channels showed robust plasma membrane localization, whereas the binding-deficient mutant was mainly localized to the cytoplasm (Fig. 5E). We also mutated this region in TRPV6 (600-5G-607) and investigated whether similar trafficking defects were displayed. In line with our results with TRPV5, wild-type TRPV6 showed significant plasma membrane staining, whereas TRPV6 600-5G-607 was absent from the plasma membrane but accumulated intracellularly (Fig. 5E). The functional role of Rab11a binding was subsequently investigated by $^{45}Ca^{2+}$ uptake measurements with oocytes. Expression of wild-type TRPV5 resulted in an ~5-fold increase in the Ca^{2+} uptake compared to noninjected oocytes, whereas expression of the TRPV5 595-5G-601 mutant resulted in a Ca^{2+} uptake that was indistinguishable from that of noninjected oocytes (Fig. 5F). Similar results were obtained

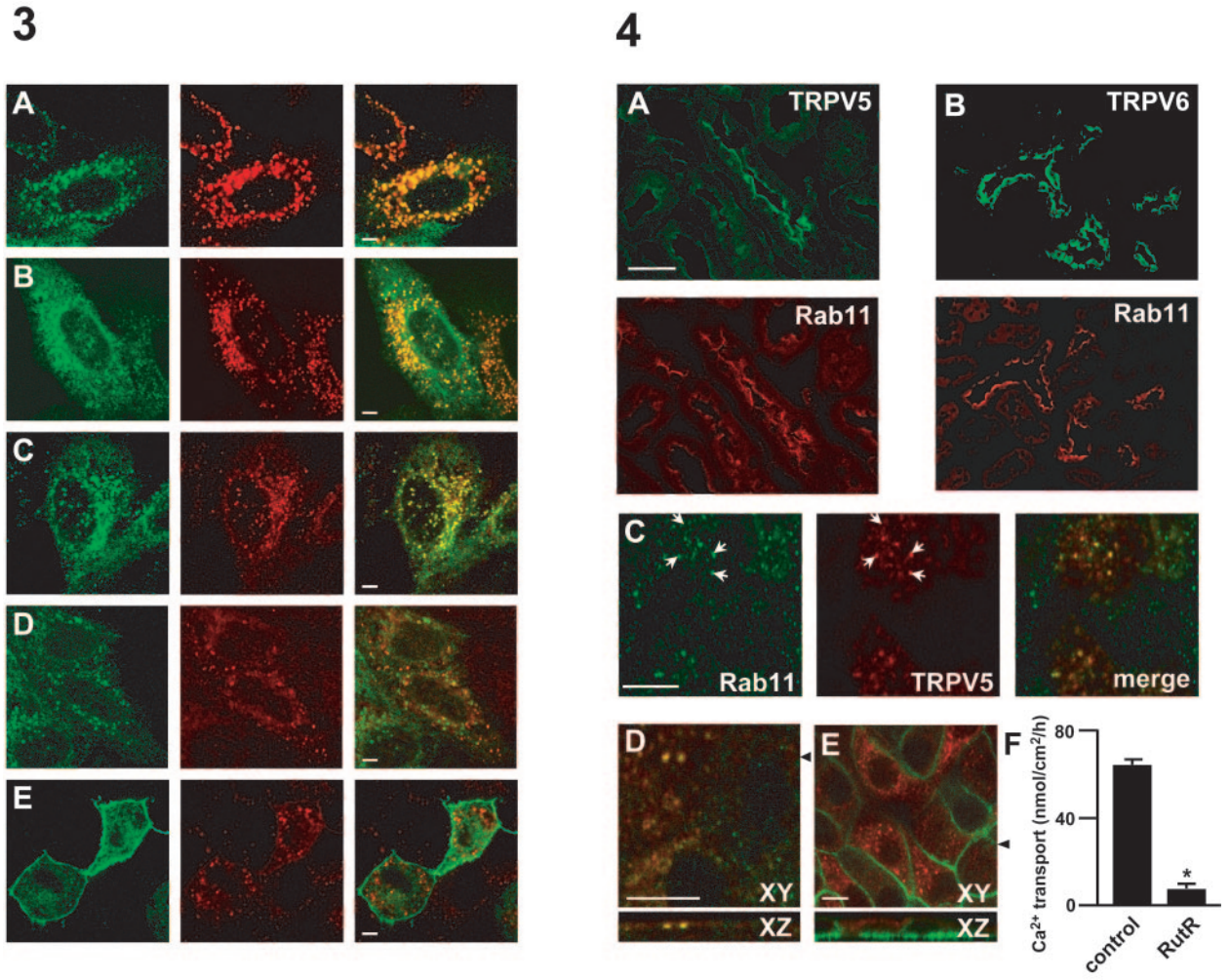

FIG. 3. Colocalization of TRPV5 with Rab11a wild type, S20V, and S25N in cytoplasmic vesicles. HeLa cells were transiently transfected with pEGFP-TRPV5 and wild-type DsRed-Rab11 (A), DsRed-Rab11a S20V (B), DsRed-Rab11a S25N (C), or DsRed-Rab4 (D). TRPV5 was mainly present in vesicles and to a lesser extent in the endoplasmic reticulum. TRPV5 (in green) completely colocalized with wild-type Rab11a (in red) in these vesicles, whereas virtually no colocalization was observed between TRPV5 and Rab4 (D). Rab11a S20V (B), as well as Rab11a S25N (C) (both in red), showed a prominent vesicular pattern that largely colocalized with TRPV5 (in green). Coexpression of YFP-TRPV2 (in green) and DsRed-Rab11a resulted in little or no overlap between the fluorescent signals (E). Bars, 5 μm.

FIG. 4. Colocalization of endogenous TRPV5 and TRPV6 with Rab11a. (A) Mouse kidney sections were costained with antibodies against TRPV5 (green) and Rab11a (red). (B) Serial kidney sections were stained with antibodies against TRPV6 (green) or Rab11a (red). Immunodissected CNT and CCD cells were grown on permeable filter supports and double labeled with anti-TRPV5 (red) and anti-Rab11 (green) (C and D) or steptavidin-Oregon green (E) to visualize the cell surface. Arrowheads indicate the positions utilized to render XZ projections from 35 confocal optical sections (0.2 μm apart). (F) Transcellular Ca^{2+} transport in control situations and in the presence of 1 μM ruthenium red was measured prior to fixation to ensure monolayer integrity and cell viability. The robust transcellular Ca^{2+} transport demonstrates the quality of the preparation. Bar, 100 μm (A and B) or 5 μm (C to E).

with TRPV6 and the TRPV6 600-5G-607 mutant (Fig. 5F). The functional significance of the identified Rab11a-binding site was further underscored by sequence conservation among all members of the epithelial Ca^{2+} channels TRPV5 and TRPV6 identified so far (Fig. 5D), ranging from humans to zebra fish (*Danio rerio*).

Rab11a S25N inhibited TRPV5- and TRPV6-mediated Ca^{2+} influx. The effect of Rab11a expression on TRPV5 and TRPV6 activity at the plasma membrane was determined with *Xenopus laevis* oocytes by a $^{45}Ca^{2+}$ uptake assay. Expression of TRPV5 and TRPV6 resulted in an ~5-fold increase of Ca^{2+} influx compared to noninjected oocytes (Fig. 6A and B). Coexpression of Rab11a S25N significantly decreased the TRPV5- and TRPV6-mediated Ca^{2+} influx to a level that was indistinguishable from that of noninjected oocytes (Fig. 6A and B). Coexpression of Rab11a S20V or Rab22b S19N had no significant effect on TRPV5 and TRPV6 activity. Ca^{2+} uptake in oocytes expressing only Rab11a S20V or Rab11a S25N was no different from that of noninjected oocytes (0.49 ± 0.07 and 0.42 ± 0.05 versus 0.44 ± 0.04 pmol Ca^{2+}/oocyte/h, respectively). The effect of Rab11a S25N was consistent with a role for Rab11a in TRPV5 and TRPV6 targeting to the plasma membrane. Therefore, we investigated trafficking of TRPV5 in *Xenopus laevis* oocytes. A distinct band at the size of complex glycosylated

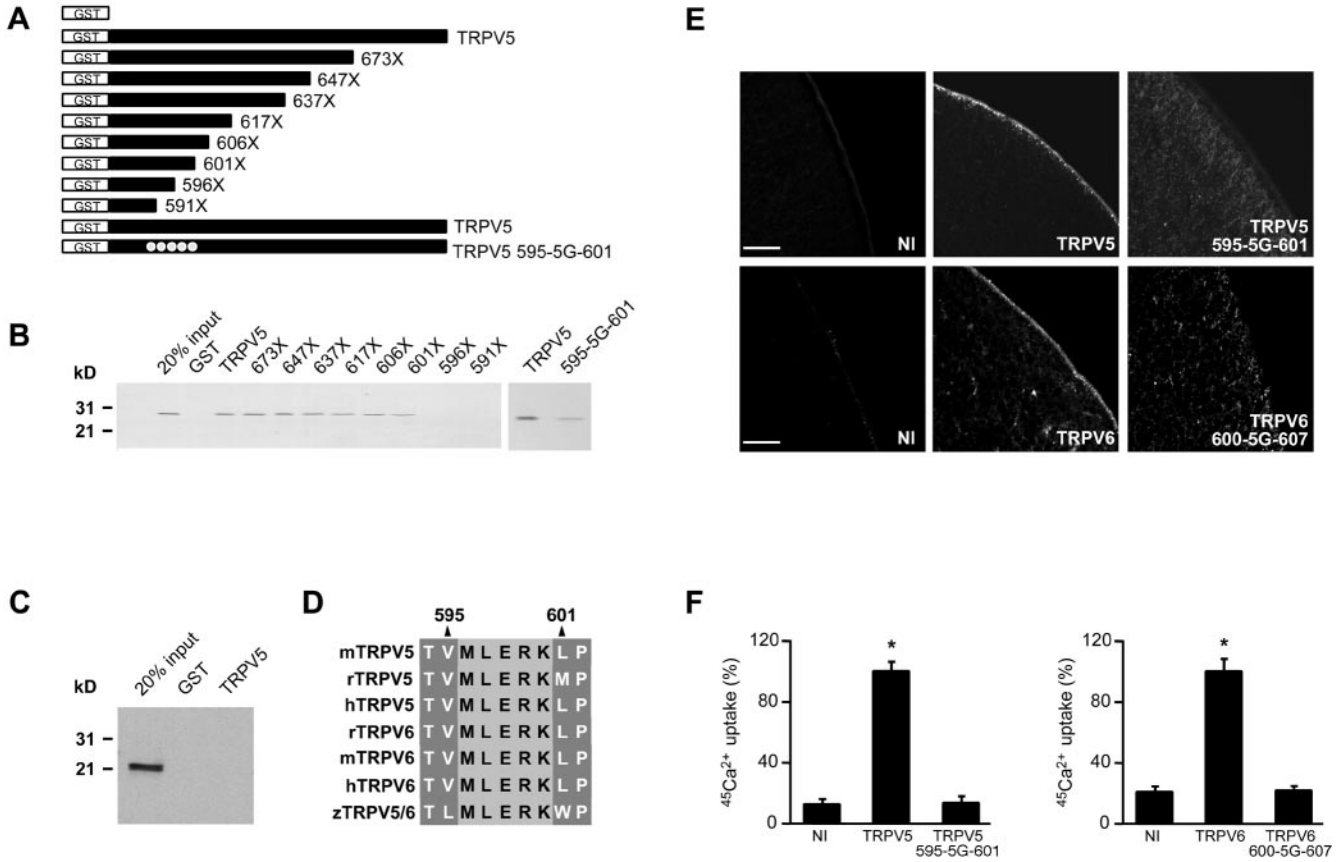

FIG. 5. Rab11a-binding site in TRPV5. (A) GST fusion proteins containing different portions of the carboxyl terminus of mouse TRPV5 were constructed according to the schematic drawing. (B) These proteins were immobilized on glutathione-Sepharose 4B beads and then incubated with in vitro-translated Rab11a S25N. Interaction of Rab11a with the GST fusion proteins was determined by autoradiography. The region between amino acids 595 and 601 was essential for binding. Mutation of this region (595-5G-601) diminished the interaction with Rab11a (right). (C) GST or GST fused to the carboxyl terminus of TRPV5 and immobilized on glutathione-Sepharose 4B beads was incubated with in vitro-translated Rab22b; precipitated proteins were analyzed by autoradiography. Rab22b did not associate with TRPV5, demonstrating the specificity of the Rab11a binding. (D) TRPV5 and TRPV6 sequences, varying from humans to zebra fish, were aligned by the Clustal method, demonstrating complete conservation of the Rab11a-binding site during evolution. (E) cRNA encoding full-length TRPV5 or TRPV6 was injected in *Xenopus laevis* oocytes, and the localization of the channel was investigated by immunocytochemistry. Mutation of five amino acids in the Rab11a-binding region resulted in significantly disturbed TRPV5/6 trafficking, resulting in a small number of channels at the cell surface. (F) Accordingly, TRPV5-mediated $^{45}Ca^{2+}$ uptake was significantly decreased in *Xenopus laevis* oocytes injected with TRPV5 595-5G-601, compared to oocytes injected with wild-type TRPV5. Similar functional results were obtained between the wild type and 600-5G-607 mutant TRPV6. Bar, 25 μm.

TRPV5 (24) was observed by immunoblot analysis of plasma membrane preparations of TRPV5-injected oocytes (Fig. 6C). The core-glycosylated form of TRPV5 was not detectable, indicating the purity of the plasma membrane preparation obtained by this method (25). Importantly, TRPV5 could not be detected in the plasma membrane of oocytes coexpressing TRPV5 and Rab11a S25N, whereas coinjection of Rab11a S20V resulted in normal plasma membrane localization of TRPV5 (Fig. 6C). In all conditions, TRPV5 was produced and glycosylated to an extent similar to that in the absence of mutant Rab11a protein (Fig. 6D). These results were verified by immunocytochemical analysis of TRPV5- and Rab11a-expressing oocytes. Immunopositive staining for TRPV5 was predominantly localized along the plasma membrane (Fig. 6E). Coinjection of TRPV5 with Rab11a S25N resulted in largely dispersed intracellular immunopositive staining with virtually no staining of TRPV5 at the plasma membrane, while expression of Rab11 S20V had no effect (Fig. 6E). The role of Rab11a in the regulation of TRPV5 was further investigated by using primary cultures of CNT/CCD cells grown to confluence on permeable filter supports. Lentivirus-mediated expression of GFP-fused Rab11a S25N or GFP only was verified by confocal laser scanning microscopy (Fig. 7A). GFP-Rab11a S25N displayed a tubulovesicular localization, while GFP showed a predominant diffuse cytosolic pattern. Rab11a S25N partially colocalized with endogenous TRPV5, whereas GFP alone showed no colocalization (Fig. 7A), in line with the colocalization results obtained with HeLa cells (Fig. 3). The expression of GFP and GFP-fused Rab11a S25N was further confirmed by immunoblot analysis using anti-GFP antibodies showing single bands of comparable intensity at the expected height for GFP and GFP-fused Rab11a S25N (Fig. 7B). Importantly, transcellular Ca^{2+} transport showed a significant and dose-dependent inhibition in Rab11a S25N-expressing primary CNT-CCD monolayers, compared to monolayers expressing GFP only. Viral infections did not affect the transepithelial resistance in

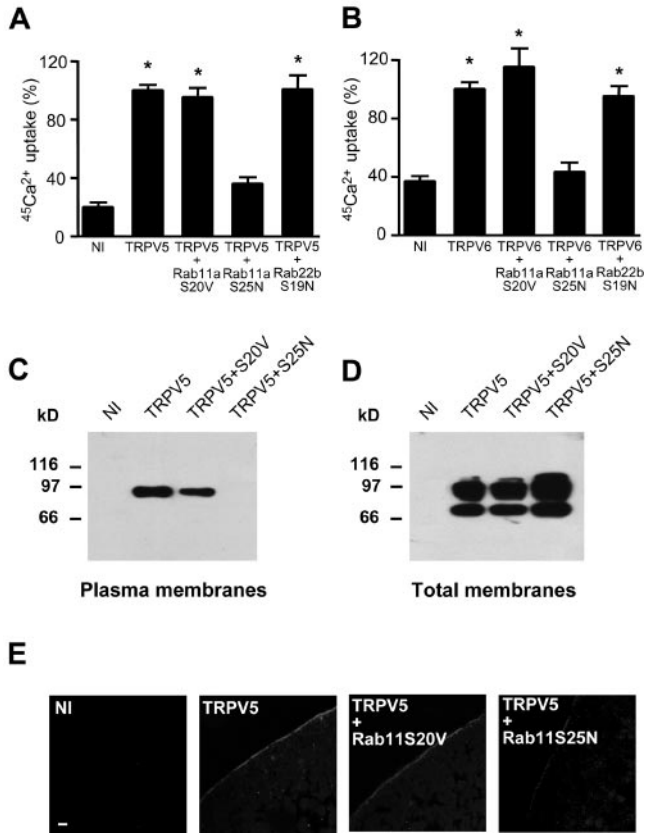

FIG. 6. Role of Rab11a in TRPV5 and TRPV6 trafficking to the plasma membrane. $^{45}Ca^{2+}$ uptake was measured in oocytes injected with TRPV5 cRNA (A) or TRPV6 cRNA (B) only or coinjected with Rab11a S20V, Rab11a S25N, or Rab22b S19N cRNA. An asterisk indicates results that were significantly ($P < 0.05$) different from noninjected oocytes. HA-TRPV5 and Rab11a cRNA were coinjected in *Xenopus laevis* oocytes. Plasma membranes (C) or total membranes (D) were isolated and blotted for TRPV5 using monoclonal anti-HA. Oocytes were injected with HA-tagged TRPV5 cRNA with or without Rab11a cRNA; TRPV5 localization was determined by immunocytochemistry using monoclonal anti-HA (E). Rab11a S25N expression decreased TRPV5 plasma membrane localization. Representative images of three independent experiments are shown. Bar, 10 μm.

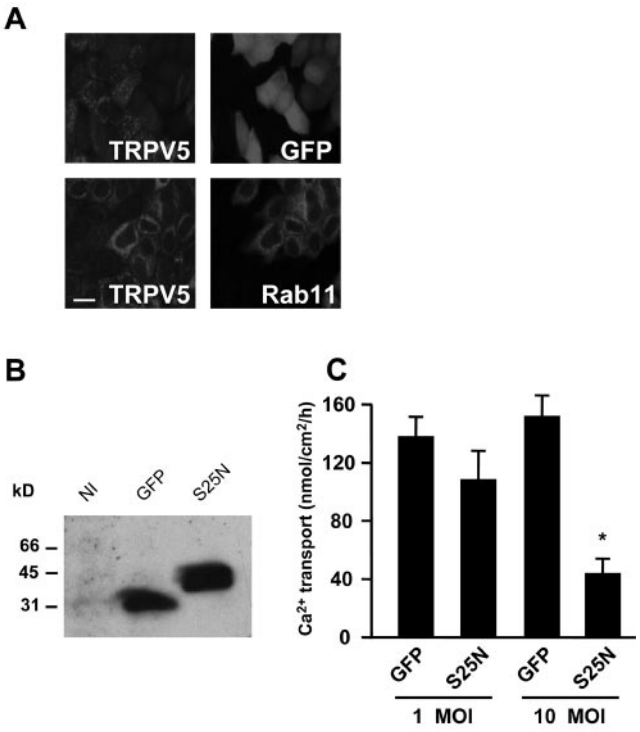

FIG. 7. Rab11a S25N inhibits transcellular Ca^{2+} transport in primary cultures of CNT-CCD cells. CNT-CCD cells were immunodissected from rabbit kidney, infected with lentivirus, and plated on permeable filter supports. Confluent monolayers of CNT-CCD cells were analyzed 6 days postinfection. (A) Expression of GFP and GFP-fused Rab11a S25N was investigated by confocal laser scanning microscopy; localization of the GFP signal was compared to endogenous TRPV5. (B) Lentiviral expression of GFP or GFP-fused Rab11a S25N was quantified by immunoblot analysis using anti-GFP antibodies confirming the size and integrity of the proteins. (C) Net apical-to-basolateral Ca^{2+} transport was measured in forskolin-stimulated (10 μM) CNT-CCD monolayers infected with lentivirus expressing either GFP alone or GFP-fused Rab11a S25N. Infections were performed at densities of 1 or 10 lentivirus particles per cell (multiplicity of infection of 1 or 10), showing a concentration-dependent inhibition of Ca^{2+} transport by Rab11a S25N (*, $P < 0.05$). NI, not infected. Bar, 10 μm.

either condition, confirming the integrity of the monolayer (not shown). Furthermore, no differences in TRPV5 expression were observed in infected versus noninfected cells. Therefore, the results obtained with the renal primary cultures were consistent with our observations using TRPV5-expressing *Xenopus* oocytes and further substantiated the role of Rab11a in the targeting of TRPV5 to the plasma membrane.

DISCUSSION

The present study demonstrates a novel function of Rab11a mediating trafficking of TRPV5 and TRPV6 to the plasma membrane by direct cargo interaction. First, GDP-bound Rab11a directly and specifically binds to a conserved stretch in the carboxyl terminus of TRPV5 and TRPV6, demonstrating a unique interaction between a TRP channel and a GDP-bound Rab. Second, the epithelial Ca^{2+} channels colocalize with Rab11a in subapical vesicles present in Ca^{2+}-transporting cells of the kidney. Third, functional data suggest that cargo interaction (in the GDP status) and subsequent GTP binding are required for Rab11a-mediated TRPV5 and TRPV6 targeting to the plasma membrane.

GDP-bound Rab11a as a novel TRPV5- and TRPV6-interacting protein. Our study describes for the first time cargo proteins that interact directly with Rab11a. Although Rab proteins are known to interact with a large variety of effectors (17, 38, 47), only a few studies have demonstrated direct interactions between a Rab GTPase and a cargo molecule (37). Recently, it was reported that the polymeric immunoglobulin A (IgA) receptor (pIgR) interacts directly with Rab3b, controlling IgA-stimulated transcytosis (42). The second example is the interaction between Rab5a and the angiotensin II type 1A receptor (34). Finally, Pfeffer and coworkers were the first to demonstrate a mechanism in which Rab proteins interact indirectly with cargo. They showed that a ternary complex of Rab9, mannose-6-phosphate receptor, and the adaptor protein TIP47 plays a role in the vesicular transport of the mannose-

6-phosphate receptor (6). Direct interaction of Rabs with cargo could provide further insight into the mechanisms of Rab localization and function. The recruitment of Rabs to specific membranes is mediated by the Rab carboxyl terminus (9). This suggests the involvement of Rab-interacting proteins in the membrane localization of Rab proteins. An intriguing possibility is that certain Rab accessory proteins are cargo themselves, contributing to the membrane localization of specific Rab proteins. As TRPV5 and TRPV6 preferentially interacted with Rab11a in its inactive configuration, TRPV5 and TRPV6 may support the recruitment of Rab11a to specific membrane compartments in Ca^{2+}-transporting epithelia. Similarly, it was suggested that the direct interaction between Rab3b and pIgR provides a partial explanation for the specificity of binding of Rab3b to pIgR-containing vesicles (42). Furthermore, direct interaction of Rabs with cargo could contribute to the targeting of proteins to their proper destination. Direct association of TRPV5/6 with Rab11a could support the translocation of these channels into recycling endosomes and thereby constitute the "delivery machinery" destined to transport these channels to the apical plasma membrane. Identification of additional novel cargo that interacts with Rab proteins could provide means to further dissect the mechanism of Rab activity and thus a novel insight into the molecular machinery of membrane traffic.

Colocalization of Rab11a and TRPV5 and TRPV6. Further evidence for a role of Rab11a in TRPV5 and TRPV6 regulation is the predominant colocalization of Rab11a with TRPV5 or TRPV6 along the apical domain of the distal convoluted tubules, CNT and CCD, corroborating previous Rab11 localization data from Goldenring et al. (15). Furthermore, Rab11a is present along the luminal membrane of enterocytes, where TRPV6 expression is prominent (15, 48). The specific expression pattern in kidney and intestine supports a role for Rab11a in the regulation of TRPV5 and TRPV6. At the subcellular level, Rab11a also shows significant colocalization with TRPV5 in subapical vesicular structures. Previous functional and histological studies have identified Rab11-positive structures as (apical) recycling endosomes, which are specialized compartments involved in (polar) sorting of endocytosed membrane proteins (5, 7, 27, 31, 45). Furthermore, Rab11 has been demonstrated to play a role in transport from the *trans*-Golgi network to the plasma membrane (33, 40). Ang and coworkers have recently demonstrated a role for recycling endosomes as intermediates in the transport from the Golgi membrane to the plasma membrane (1). Our study is the first to indicate that cargo molecules that travel via these Rab11-enriched structures can be directly bound to Rab11a.

Rab11a binding targets TRPV5 and TRPV6 to the plasma membrane. The unique role of Rab11a in targeting of TRPV5 and TRPV6 to the plasma membrane by direct interaction to the channel was further established by combined biochemical, functional, and immunocytochemical analyses. To identify the direct consequences of Rab11a association with the epithelial Ca^{2+} channels, we mutated the Rab11a-binding site in TRPV5 and TRPV6. The interaction between Rab11a and TRPV5/6 was localized to a helical stretch in the carboxyl terminus. A stretch of five amino acids at position 595 to 601 within the Rab11a-binding site of TRPV5 was demonstrated to be required for Rab11a binding. Moreover, this region is conserved among all identified species of TRPV5 and TRPV6. Mutations in this stretch resulted in a lack of TRPV5- and TRPV6-mediated Ca^{2+} uptake, based on defective trafficking of TRPV5 and TRPV6, in line with an essential role for Rab11a in targeting TRPV5/6 to the plasma membrane. However, as this stretch has been implicated in the interaction of TRPV5 with 80K-H, a Ca^{2+}-binding protein (14) and in TRPV5 channel assembly (8), Rab11a-independent factors cannot be excluded to explain the impaired trafficking of this mutant. Therefore, we further substantiated the functional role of Rab11a in the trafficking of TRPV5 and TRPV6 using Rab11a mutants in *Xenopus* oocytes and primary cultures of Ca^{2+}-transporting cells from rabbit kidney. GDP-locked Rab11a expression strongly reduced the TRPV5- and TRPV6-mediated Ca^{2+} influx, resulting from a significantly decreased number of Ca^{2+} channels at the plasma membrane. This effect can be explained in two ways. First, in analogy with dominant negative Ras mutants (13), Rab11a S25N could sequester a Rab11a guanine nucleotide exchange factor (GEF) and thereby block the activation of Rabs. However, expression of another dominant negative Rab protein (Rab22b S19N) did not inhibit TRPV5/6 activity. This suggests either that Rab GEF inhibition is not essential to block TRPV5/6 trafficking or that Rab11a S25N associates with a specific GEF that does not bind Rab22b S19N. It is currently unknown which protein operates as a GEF for Rab11a and how promiscuous this GEF is. Rab11a S20V has a lower affinity for Rab GEFs (10, 45), explaining the lack of functional consequences of expression of

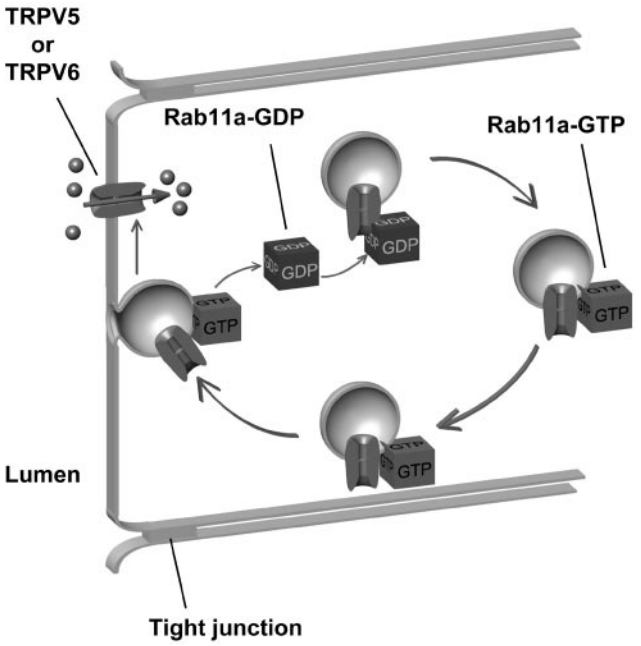

FIG. 8. Schematic model depicting the role of Rab11a in TRPV5 and TRPV6 trafficking. Rab11a-GDP interacts directly with TRPV5 or TRPV6 in intracellular vesicles. Subsequently, Rab11a is docked at the vesicle, and GDP is exchanged for GTP. Several Rab effectors stabilize Rab11a in the membrane in the GTP-bound state. At this state, Rab11a no longer interacts with TRPV5 or TRPV6. The vesicle is subsequently targeted to the plasma membrane, where its fusion enables TRPV5- and TRPV6-mediated Ca^{2+} influx.

this mutant. Second, the dominant negative effect of Rab11a S25N could be explained as a competition with endogenous Rab11a for the Rab11a-binding site in TRPV5/6. Because Rab11a S25N cannot bind GTP, it will not be activated, and this impairs TRPV5/6 trafficking to the plasma membrane. Rab11a S20V cannot compete with endogenous Rab11a for TRPV5/6 binding, explaining the lack of function of this mutant. Together, these data indicate that cargo interaction (in the GDP status), as well as subsequent GTP binding, is required for Rab11a-mediated TRPV5/6 trafficking. Our findings show a novel interaction between a Rab GTPase and TRP channels and point to a unique role for Rab11a in the regulation of TRPV5/6 channel trafficking.

We propose the following model for the role of Rab11a in trafficking of TRPV5 and TRPV6 (Fig. 8). Initially, cytosolic GDP-bound Rab11a specifically interacts with TRPV5 and TRPV6 in a cytoplasmic compartment. Subsequently, Rab11a is docked to this compartment, while GDP is exchanged with GTP. At this state, Rab11a effectors will associate, and Rab11a no longer interacts with TRPV5 and TRPV6. Finally, active GTP-bound Rab11a mediates transport of TRPV5- and TRPV6-containing structures to the plasma membrane, where membrane fusion allows Ca^{2+} influx.

In conclusion, our data provide new insight into the molecular machinery of TRP channel trafficking via direct interaction between a Rab GTPase and apically targeted cargo. This association is involved in the physiological regulation of TRPV5 and TRPV6 cell surface abundance, a critical component in Ca^{2+} homeostasis. The future challenge is to find the signals that modulate the interaction of TRPV5/6 and Rab11a to fine-tune cell surface expression of these epithelial channels.

ACKNOWLEDGMENTS

We thank R. C. Hoeben and L. Boele (LUMC, Leiden, The Netherlands) for kindly providing the lentivirus transfer vector and advice on virus production and infections and O. Brouwers for excellent technical assistance. We are grateful to J. Fransen (NCMLS, Nijmegen, The Netherlands) for discussions and J. Neefjes (NKI, Amsterdam, The Netherlands), M. Schaefer (Institut für Pharmakologie, Berlin, Germany), and U. Rescher (ZMBE, Muenster, Germany) for providing constructs.

This work was supported by the Dutch Organization of Scientific Research (Zon-Mw 016.006.001 and NWO Talent S91-282) and the Human Frontier Science Program (RGP 32/2004).

REFERENCES

1. **Ang, A. L., T. Taguchi, S. Francis, H. Folsch, L. J. Murrells, M. Pypaert, G. Warren, and I. Mellman.** 2004. Recycling endosomes can serve as intermediates during transport from the Golgi to the plasma membrane of MDCK cells. J. Cell Biol. **167:**531–543.
2. **Bahner, M., S. Frechter, N. Da Silva, B. Minke, R. Paulsen, and A. Huber.** 2002. Light-regulated subcellular translocation of *Drosophila* TRPL channels induces long-term adaptation and modifies the light-induced current. Neuron **34:**83–93.
3. **Bezzerides, V. J., I. S. Ramsey, S. Kotecha, A. Greka, and D. E. Clapham.** 2004. Rapid vesicular translocation and insertion of TRP channels. Nat. Cell Biol. **6:**709–720.
4. **Brewer, C. B., and M. G. Roth.** 1991. A single amino acid change in the cytoplasmic domain alters the polarized delivery of influenza virus hemagglutinin. J. Cell Biol. **114:**413–421.
5. **Brown, P. S., E. Wang, B. Aroeti, S. J. Chapin, K. E. Mostov, and K. W. Dunn.** 2000. Definition of distinct compartments in polarized Madin-Darby canine kidney (MDCK) cells for membrane-volume sorting, polarized sorting and apical recycling. Traffic **1:**124–140.
6. **Carroll, K. S., J. Hanna, I. Simon, J. Krise, P. Barbero, and S. R. Pfeffer.** 2001. Role of Rab9 GTPase in facilitating receptor recruitment by TIP47. Science **292:**1373–1376.
7. **Casanova, J. E., X. Wang, R. Kumar, S. G. Bhartur, J. Navarre, J. E. Woodrum, Y. Altschuler, G. S. Ray, and J. R. Goldenring.** 1999. Association of Rab25 and Rab11a with the apical recycling system of polarized Madin-Darby canine kidney cells. Mol. Biol. Cell **10:**47–61.
8. **Chang, Q., E. Gyftogianni, S. F. van de Graaf, S. Hoefs, F. A. Weidema, R. J. Bindels, and J. G. Hoenderop.** 2004. Molecular determinants in TRPV5 channel assembly. J. Biol. Chem. **279:**54304–54311.
9. **Chavrier, P., J. P. Gorvel, E. Stelzer, K. Simons, J. Gruenberg, and M. Zerial.** 1991. Hypervariable C-terminal domain of rab proteins acts as a targeting signal. Nature **353:**769–772.
10. **Cool, R. H., G. Schmidt, C. U. Lenzen, H. Prinz, D. Vogt, and A. Wittinghofer.** 1999. The Ras mutant D119N is both dominant negative and activated. Mol. Cell. Biol. **19:**6297–6305.
11. **de Renzis, S., B. Sonnichsen, and M. Zerial.** 2002. Divalent Rab effectors regulate the sub-compartmental organization and sorting of early endosomes. Nat. Cell Biol. **4:**124–133.
12. **Dull, T., R. Zufferey, M. Kelly, R. J. Mandel, M. Nguyen, D. Trono, and L. Naldini.** 1998. A third-generation lentivirus vector with a conditional packaging system. J. Virol. **72:**8463–8471.
13. **Farnsworth, C. L., and L. A. Feig.** 1991. Dominant inhibitory mutations in the Mg^{2+}-binding site of RasH prevent its activation by GTP. Mol. Cell. Biol. **11:**4822–4829.
14. **Gkika, D., F. Mahieu, B. Nilius, J. G. Hoenderop, and R. J. Bindels.** 2004. 80K-H as a new Ca^{2+} sensor regulating the activity of the epithelial Ca^{2+} channel transient receptor potential cation channel V5 (TRPV5). J. Biol. Chem. **279:**26351–26357.
15. **Goldenring, J. R., J. Smith, H. D. Vaughan, P. Cameron, W. Hawkins, and J. Navarre.** 1996. Rab11 is an apically located small GTP-binding protein in epithelial tissues. Am. J. Physiol. **270:**G515–G525.
16. **Gonzalez, L., Jr., and R. H. Scheller.** 1999. Regulation of membrane trafficking: structural insights from a Rab/effector complex. Cell **96:**755–758.
17. **Hales, C. M., R. Griner, K. C. Hobdy-Henderson, M. C. Dorn, D. Hardy, R. Kumar, J. Navarre, E. K. Chan, L. A. Lapierre, and J. R. Goldenring.** 2001. Identification and characterization of a family of Rab11-interacting proteins. J. Biol. Chem. **276:**39067–39075.
18. **Hoenderop, J. G., A. Hartog, M. Stuiver, A. Doucet, P. H. Willems, and R. J. Bindels.** 2000. Localization of the epithelial Ca^{2+} channel in rabbit kidney and intestine. J. Am. Soc. Nephrol. **11:**1171–1178.
19. **Hoenderop, J. G., B. Nilius, and R. J. Bindels.** 2002. Molecular mechanism of active Ca^{2+} reabsorption in the distal nephron. Annu. Rev. Physiol. **64:**529–549.
20. **Hoenderop, J. G., A. B. Vaandrager, L. Dijkink, A. Smolenski, S. Gambaryan, S. M. Lohmann, H. R. de Jonge, P. H. Willems, and R. J. Bindels.** 1999. Atrial natriuretic peptide-stimulated Ca^{2+} reabsorption in rabbit kidney requires membrane-targeted, cGMP-dependent protein kinase type II. Proc. Natl. Acad. Sci. USA **96:**6084–6089.
21. **Hoenderop, J. G., A. W. van der Kemp, A. Hartog, S. F. van de Graaf, C. H. van Os, P. H. Willems, and R. J. Bindels.** 1999. Molecular identification of the apical Ca^{2+} channel in 1, 25-dihydroxyvitamin D_3-responsive epithelia. J. Biol. Chem. **274:**8375–8378.
22. **Hoenderop, J. G., A. W. van der Kemp, A. Hartog, C. H. van Os, P. H. Willems, and R. J. Bindels.** 1999. The epithelial calcium channel, ECaC, is activated by hyperpolarization and regulated by cytosolic calcium. Biochem. Biophys. Res. Commun. **261:**488–492.
23. **Hoenderop, J. G., J. P. van Leeuwen, B. C. van der Eerden, F. F. Kersten, A. W. van der Kemp, A. M. Merillat, J. H. Waarsing, B. C. Rossier, V. Vallon, E. Hummler, and R. J. Bindels.** 2003. Renal Ca^{2+} wasting, hyperabsorption, and reduced bone thickness in mice lacking TRPV5. J. Clin. Investig. **112:**1906–1914.
24. **Hoenderop, J. G., T. Voets, S. Hoefs, F. Weidema, J. Prenen, B. Nilius, and R. J. Bindels.** 2003. Homo- and heterotetrameric architecture of the epithelial Ca^{2+} channels TRPV5 and TRPV6. EMBO J. **22:**776–785.
25. **Kamsteeg, E. J., and P. M. Deen.** 2001. Detection of aquaporin-2 in the plasma membranes of oocytes: a novel isolation method with improved yield and purity. Biochem. Biophys. Res. Commun. **282:**683–690.
26. **Kanzaki, M., Y. Q. Zhang, H. Mashima, L. Li, H. Shibata, and I. Kojima.** 1999. Translocation of a calcium-permeable cation channel induced by insulin-like growth factor-I. Nat. Cell Biol. **1:**165–170.
27. **Leung, S. M., W. G. Ruiz, and G. Apodaca.** 2000. Sorting of membrane and fluid at the apical pole of polarized Madin-Darby canine kidney cells. Mol. Biol. Cell **11:**2131–2150.
28. **Montell, C., L. Birnbaumer, and V. Flockerzi.** 2002. The TRP channels, a remarkably functional family. Cell **108:**595–598.
29. **Nijenhuis, T., J. G. Hoenderop, A. W. van der Kemp, and R. J. Bindels.** 2003. Localization and regulation of the epithelial Ca^{2+} channel TRPV6 in the kidney. J. Am. Soc. Nephrol. **14:**2731–2740.
30. **Nilius, B., J. Prenen, R. Vennekens, J. G. Hoenderop, R. J. Bindels, and G. Droogmans.** 2001. Pharmacological modulation of monovalent cation currents through the epithelial Ca^{2+} channel ECaC1. Br. J. Pharmacol. **134:**453–462.

31. **Prekeris, R., J. Klumperman, and R. H. Scheller.** 2000. A Rab11/Rip11 protein complex regulates apical membrane trafficking via recycling endosomes. Mol. Cell **6:**1437–1448.
32. **Ren, M., G. Xu, J. Zeng, C. De Lemos-Chiarandini, M. Adesnik, and D. D. Sabatini.** 1998. Hydrolysis of GTP on rab11 is required for the direct delivery of transferrin from the pericentriolar recycling compartment to the cell surface but not from sorting endosomes. Proc. Natl. Acad. Sci. USA **95:** 6187–6192.
33. **Satoh, A. K., J. E. O'Tousa, K. Ozaki, and D. F. Ready.** 2005. Rab11 mediates post-Golgi trafficking of rhodopsin to the photosensitive apical membrane of *Drosophila* photoreceptors. Development **132:**1487–1497.
34. **Seachrist, J. L., S. A. Laporte, L. B. Dale, A. V. Babwah, M. G. Caron, P. H. Anborgh, and S. S. Ferguson.** 2002. Rab5 association with the angiotensin II type 1A receptor promotes Rab5 GTP binding and vesicular fusion. J. Biol. Chem. **277:**679–685.
35. **Seppen, J., M. Rijnberg, M. P. Cooreman, and R. P. Oude Elferink.** 2002. Lentiviral vectors for efficient transduction of isolated primary quiescent hepatocytes. J. Hepatol. **36:**459–465.
36. **Singh, B. B., T. P. Lockwich, B. C. Bandyopadhyay, X. Liu, S. Bollimuntha, S. C. Brazer, C. Combs, S. Das, A. G. Leenders, Z. H. Sheng, M. A. Knepper, S. V. Ambudkar, and I. S. Ambudkar.** 2004. VAMP2-dependent exocytosis regulates plasma membrane insertion of TRPC3 channels and contributes to agonist-stimulated Ca^{2+} influx. Mol. Cell **15:**635–646.
37. **Smythe, E.** 2002. Direct interactions between rab GTPases and cargo. Mol. Cell **9:**205–206.
38. **Stenmark, H., G. Vitale, O. Ullrich, and M. Zerial.** 1995. Rabaptin-5 is a direct effector of the small GTPase Rab5 in endocytic membrane fusion. Cell **83:**423–432.
39. **Ullrich, O., S. Reinsch, S. Urbe, M. Zerial, and R. G. Parton.** 1996. Rab11 regulates recycling through the pericentriolar recycling endosome. J. Cell Biol. **135:**913–924.
40. **Urbe, S., L. A. Huber, M. Zerial, S. A. Tooze, and R. G. Parton.** 1993. Rab11, a small GTPase associated with both constitutive and regulated secretory pathways in PC12 cells. FEBS Lett. **334:**175–182.
41. **Van de Graaf, S. F., J. G. Hoenderop, D. Gkika, D. Lamers, J. Prenen, U. Rescher, V. Gerke, O. Staub, B. Nilius, and R. J. Bindels.** 2003. Functional expression of the epithelial Ca^{2+} channels (TRPV5 and TRPV6) requires association of the S100A10-annexin 2 complex. EMBO J. **22:** 1478–1487.
42. **Van IJzendoorn, S. C., M. J. Tuvim, T. Weimbs, B. F. Dickey, and K. E. Mostov.** 2002. Direct interaction between Rab3b and the polymeric immunoglobulin receptor controls ligand-stimulated transcytosis in epithelial cells. Dev. Cell **2:**219–228.
43. **Vennekens, R., J. G. Hoenderop, J. Prenen, M. Stuiver, P. H. Willems, G. Droogmans, B. Nilius, and R. J. Bindels.** 2000. Permeation and gating properties of the novel epithelial Ca^{2+} channel. J. Biol. Chem. **275:**3963–3969.
44. **Wakabayashi, Y., J. Lippincott-Schwartz, and I. M. Arias.** 2004. Intracellular trafficking of bile salt export pump (ABCB11) in polarized hepatic cells: constitutive cycling between the canalicular membrane and rab11-positive endosomes. Mol. Biol. Cell **15:**3485–3496.
45. **Wang, X., R. Kumar, J. Navarre, J. E. Casanova, and J. R. Goldenring.** 2000. Regulation of vesicle trafficking in Madin-Darby canine kidney cells by Rab11a and Rab25. J. Biol. Chem. **275:**29138–29146.
46. **Xu, X. Z., F. Moebius, D. L. Gill, and C. Montell.** 2001. Regulation of melastatin, a TRP-related protein, through interaction with a cytoplasmic isoform. Proc. Natl. Acad. Sci. USA **98:**10692–10697.
47. **Zerial, M., and H. McBride.** 2001. Rab proteins as membrane organizers. Nat Rev. Mol. Cell Biol. **2:**107–117.
48. **Zhuang, L., J. B. Peng, L. Tou, H. Takanaga, R. M. Adam, M. A. Hediger, and M. R. Freeman.** 2002. Calcium-selective ion channel, CaT1, is apically localized in gastrointestinal tract epithelia and is aberrantly expressed in human malignancies. Lab. Investig. **82:**1755–1764.